Influence of Chemical and Electrostatic Gradients on Diffusion in Microemulsions

Robert J. McGreevy and Robert S. Schechter
Dept. of Chemical Engineering, University of Texas, Austin, TX 78712

Nonequilibrium diffusion behavior in nonionic and ionic surfactant microemulsion systems has been studied experimentally using the open-ended capillary method. Experimental results for these systems have been compared with a drop theory of diffusion for microemulsions under conditions where large concentration and electrostatic gradients exist. The results show good agreement in concentration profiles between theory and experiment for the microemulsion components—water, benzene, and phenol. Furthermore, under certain conditions the theory predicts that over a limited time interval phenol will diffuse from low-concentration regions to regions of higher concentration. This phenomenon has been observed.

Introduction

Microemulsions are of considerable scientific and industrial importance and have in recent years become the focus of much research (Ekwall, 1975; Luisi and Straub, 1984; Bourrel and Schechter, 1988). The study of diffusion in microemulsions and surfactant solutions has appeared prominently in the literature because diffusion coefficients are necessary for describing mass transfer in these systems and also because diffusion data can be used to probe their microstructure. Papers dealing with diffusion in microemulsions fall into two categories, self-diffusion and nonequilibrium diffusion. Self-diffusion refers to the random movement of tagged particles at equilibrium in the absence of concentration gradients. Nonequilibrium or mutual diffusion also describes random movement of particles, but under the condition of bulk gradients in which there is a net transfer of matter over space and time. The former category of diffusion studies is by far the more predominant. It includes the Fourier transform NMR investigations pioneered by Stilbs, Lindman, and their coworkers (Lindman et al., 1981; Stilbs and Lindman, 1984). Other methods used to study self-diffusion include the use of radioactive isotope tracers (Lam and Schechter, 1987a) and dyes solubilized inside swollen micelles (Armstrong et al., 1988). By comparison, diffusion studies of microemulsions in the presence of large concentration gradients are relatively scarce. Notable examples of this category are papers by Benton et al. (1986) and Raney and Miller (1987), which employ diffusion path theory to study mass transfer and the formation of intermediate phases when aqueous surfactant solutions are contacted with oil. Experiments using videomicroscopy techniques also allowed these investigators to view intermediate phase growth, interface motion, and spontaneous emulsification. Nonequilibrium diffusion results are directly applicable to diffusional processes that result from concentration gradients, which can be found in industrial applications such as enhanced oil recovery and detergency.

The aim of the present work is to extend the predictions of the droplet diffusion model (Lam and Schechter, 1987b) to include the more general case of nonequilibrium diffusion, when microemulsions of unlike composition are contacted. In this paper, an experimental study of nonequilibrium diffusion in nonionic and ionic microemulsion systems is compared with theoretical predictions based on the theory of diffusion. The selection of these microemulsion systems permits the effects of concentration and electrostatic gradients to be examined separately and compared.

Theory

Droplet model

Lam and Schechter (1987b) have modeled the nonequilibrium behavior of microemulsion systems that have a spherical droplet microstructure, where noninteracting droplets are dispersed in a continuous phase. A component i in the microemulsion may be found in the continuous phase or the droplet phase, or it may partition between them. Local equilibrium of component i is assumed, in which the exchange of matter

Correspondence concerning this paper should be addressed to R. S. Schechter.
The present address of R. J. McGreevy is Monsanto Chemical Co., Springfield, MA 01151.

between the continuous and droplet phases occurs on a time scale much faster than diffusion. The flux of component i which resides in the continuous phase is

$$-J_i^f = D_i(1-\phi_d)^2\nabla C_i^f + \frac{eZ_iD_i(1-\phi_d)^2C_i^f}{kT}\nabla\psi \quad (1)$$

In this expression, D_i is the molecular diffusivity of component i, ϕ_d is the volume fraction of the dispersed phase, C_i^f is the concentration of component i in the continuous phase, Z_i is the valence of component i, ψ is the electrical potential, and the operator ∇ is the gradient. The term $(1-\phi_d)^2$ is the obstruction factor (Lam and Schechter, 1987b), which accounts for the hindering of continuous-phase diffusion due to the presence of droplets. The flux of droplets in the dispersed phase is

$$-J_m = D_m\nabla C_m + \frac{eZ_mD_mC_m}{kT}\nabla\psi \quad (2)$$

where D_m is the diffusion coefficient of the Brownian droplets, C_m is the concentration of droplets per volume of microemulsion, and Z_m is the net valence of the droplets. The volume of a spherical droplet is $(4\pi R^3/3)$, where R is the radius. Since each droplet carries with it C_i^d moles of component i per droplet volume, the flux of component i associated with the dispersed phase is

$$-J_{mi} = D_m\nabla\left[\left(\frac{4\pi R^3}{3}\right)C_mC_i^d\right] + \frac{eZ_mD_m}{kT}\left[\left(\frac{4\pi R^3}{3}\right)C_mC_i^d\right]\nabla\psi \quad (3)$$

The total flux of component i in the microemulsion is the sum of the continuous and dispersed phase portions

$$J_i^T = J_i^f + J_{mi} \quad (4)$$

The total flux J_i^T relates directly to the effective diffusion coefficient for component i that one would observe experimentally. In the case of tracer diffusion, a closed-form expression for this diffusion coefficient may be obtained from the theory (Lam and Schechter, 1987b).

Analysis of nonequilibrium diffusion

In the general case where microemulsions of unlike composition are brought into contact, the diffusion problem is a nonlinear one due to bulk gradients of droplet volume fraction ϕ_d and electrical potential ψ. It is not possible to obtain a closed-form solution for this case. To calculate diffusion, one must solve the mass continuity equations for components i subject to appropriate boundary conditions. In this section, the model is developed further so that a numerical simulation of a selected diffusion experiment is feasible. The purpose of the analysis that follows is to derive expressions for all variables found in the diffusional fluxes, so that they may be expressed in terms of two system-dependent variables: C_i, which is the total concentration of component i per volume of microemulsion, and droplet volume fraction ϕ_d. On the basis of a thermodynamic theory of microemulsions (Miller and Neogi, 1980; Huh, 1983; Ruckenstein, 1978; Overbeek, 1978), ϕ_d and R are determined by local equilibrium.

The total concentration C_i accounts for component i located in both the continuous and dispersed phases, and it may be expressed in a mass balance, which contains the other concentration variables

$$C_i = (1-\phi_d)C_i^f + \phi_dC_i^d \quad (5)$$

The fraction of component i located in the continuous phase may be defined as α_i:

$$\alpha_i = \frac{C_i^f(1-\phi_d)}{C_i} \quad (6)$$

This factor can in turn be expressed in terms of β_i, the thermodynamic partition factor for component i between the continuous and dispersed phases. For the systems studied here, the partition factor is essentially a constant and is expressed as

$$\beta_i = \frac{C_i^d}{C_i^f} \quad (7)$$

Substitution of these relations allows us to express the fraction of component i in the continuous phase as

$$\alpha_i = \frac{(1-\phi_d)}{(1-\phi_d)+\beta_i\phi_a} \quad (8)$$

These relationships permit us to express the fluxes explicitly in terms of total concentration of component i, which can be measured macroscopically. In addition, droplet concentration C_m can be related to dispersed-phase volume fraction by the equation

$$\phi_d = \left(\frac{4\pi R^3}{3}\right)C_m \quad (9)$$

By making substitutions using Eq. 6, we can rewrite the flux expression for component i in the continuous phase

$$-J_i^f = D_i(1-\phi_d)^2\nabla\left[\frac{\alpha_i}{(1-\phi_d)}C_i\right] + \frac{eZ_iD_i(1-\phi_d)}{kT}(\alpha_iC_i)\nabla\psi \quad (10)$$

Substitutions involving Eqs. 6 and 9 will lead to the following expression for flux of component i associated with movement of the dispersed phase

$$-J_{mi} = D_m\nabla[(1-\alpha_i)C_i] + \frac{eZ_mD_m}{kT}(1-\alpha_i)C_i\nabla\psi \quad (11)$$

At this juncture we assume that R is constant with respect to position and time. This assumption is a good one for the range of system variables considered here; however, for more concentrated microemulsions R may vary from point to point

and its value must be determined by applying thermodynamic arguments or the droplet morphology may not apply at all. In this latter case, a satisfactory method for calculating diffusion does not exist now.

Multiply both sides of the droplet flux equation, Eq. 2, by the volume of a droplet ($4\pi R^3/3$), to obtain a new flux equation for the dispersed phase

$$-J_d = D_m \nabla \phi_d + \frac{eZ_m D_m \phi_d}{kT} \nabla \psi \tag{12}$$

Equations 2 and 12 are equivalent in the case where R is constant. There are now two dependent variables, C_i, which is total concentration of component i, and ϕ_d, the dispersed-phase volume fraction. The gradient of electrical potential, $\nabla \psi$, may exist when ionic species are present in the microemulsion. To resolve this term, we may use the constraint of zero current

$$0 = \sum_j Z_j J_j \tag{13}$$

where the subscript j refers to the ionic diffusion species in the system. When considering an ionic surfactant microemulsion in the absence of added electrolyte, the diffusing ionic species are the surfactant monomer, the surfactant counterion, and the droplets, which have a net charge due to counterion dissociation. The fluxes of surfactant monomer and counterion are, respectively,

$$-J_s^f = D_s^f (1 - \phi_d)^2 \nabla (C_s^f N_A) + \left[\frac{eZ_s^f D_s^f C_s^f N_A (1 - \phi_d)^2}{kT}\right] \nabla \psi \tag{14}$$

$$-J_c^f = D_c^f (1 - \phi_d)^2 \nabla (C_c^f N_A) + \left[\frac{eZ_c^f D_c^f C_c^f N_A (1 - \phi_d)^2}{kT}\right] \nabla \psi \tag{15}$$

where D_s^f is the surfactant monomer diffusivity, D_c^f is the counterion diffusivity, Z_s^f is the valence of surfactant monomer, Z_c^f is the valence of the counterion, C_s^f is the surfactant monomer concentration in the continuous phase, and C_c^f is the counterion concentration in the continuous phase. Avogadro's number, N_A, is included in these expressions so that the concentration units are given in terms of the number of molecules or particles per volume, rather than in moles of particles per volume. By substituting the ionic flux expressions, Eqs. 2, 14, and 15, into Eq. 13, and rearranging, we obtain for the electrical potential gradient in a droplet microemulsion:

$$\nabla \psi = \frac{-kT}{e} \times \left[\frac{Z_c^f D_c^f (1-\phi_d)^2 N_A \nabla C_c^f + Z_m D_m \nabla C_m}{(Z_s^f)^2 D_s^f (1-\phi_d)^2 N_A C_s^f + (Z_c^f)^2 D_c^f (1-\phi_d)^2 N_A C_c^f + Z_m^2 D_m C_m}\right] \tag{16}$$

This expression reveals that the gradient of electrical potential depends on droplet concentration C_m, counterion concentration in the continuous phase C_c^f, and droplet valence Z_m. These terms are themselves functions with respect to position and time, which can be expressed in terms of droplet volume fraction ϕ_d. The other concentration term given in Eq. 16 is C_s^f, the surfactant monomer concentration in the continuous phase, which is constant and equal to the critical micelle concentration.

To simplify the numerical calculations, the variable terms in Eq. 16 will be expressed as a function of droplet volume fraction. It is also convenient to introduce the parameter A_s, the area occupied by a surfactant molecule, Thus,

$$(4\pi R^2)\, C_m = A_s C_s \tag{17}$$

where A_s is the area occupied by one mole of surfactant head groups at the droplet interface. A_s is essentially a constant for a given microemulsion system (Shulman et al., 1959). A mass balance for surfactant may be written as

$$C_s = C_s^f [1 + \phi_d (\beta_s - 1)] \tag{18}$$

where β_s is the surfactant partition factor defined in Eq. 7. It can be demonstrated (McGreevy, 1989) that a constant β_s follows as a consequence of constant droplet radius. By substituting Eq. 18 into Eq. 17, Eq. 17 into Eq. 9, and rearranging terms, we obtain this expression for droplet concentration

$$C_m = \frac{\{A_s C_s^f [1 + \phi_d (\beta_s - 1)]\}^3}{36\pi \phi_d^2} \tag{19}$$

Equation 19 expresses the droplet concentration in terms of only one variable, ϕ_d. In deriving it, we have assumed spherical droplet geometry; constant droplet radius, R; constant interfacial area per surfactant molecule, A_s; and constant surfactant monomer concentration, C_s^f, which is negligible when compared to total surfactant concentration.

Another variable term in Eq. 16 which must be analyzed is droplet valence Z_m, defined as

$$Z_m = \alpha n \tag{20}$$

where n is surfactant aggregation number in units of molecules per droplet and α is the degree of counterion dissociation from the aggregates, which depends on the molecular structure of the surfactant.

Based on Eqs. 18 and 19, Eq. 20 becomes

$$Z_m = \frac{\alpha \beta_s C_s^f N_A \phi_d}{C_m} \tag{21}$$

By using the condition of electroneutrality $\Sigma Z_j C_j = 0$, we may write a relationship for this C_c^f in terms of droplet concentration and droplet valence. Since the functionality for C_m and Z_m are known, the final expression for counterion concentration is

$$C_c^f = C_s^f + \frac{Z_m C_m}{N_A (1 - \phi_d)} \tag{22}$$

With these derivations, all the known variables found in the theory of diffusion have been completely specified; thus, the problem is ready for numerical simulation.

Simulation of nonequilibrium diffusion

Thus, the diffusion problem for microemulsions under nonequilibrium conditions is reduced to a system of two coupled nonlinear partial differential equations, which must be solved numerically subject to appropriate boundary conditions. Because of the simplicity of modeling in one-space dimension, the open-ended capillary technique of Anderson and Saddington (1949) was chosen as the experimental technique for this study. This procedure is ideally suited for studying diffusion in microemulsions.

When two microemulsions of unequal composition are brought into contact, the composition of component i in the system is governed by its continuity equation

$$\frac{\partial C_i}{\partial t} = -\nabla \cdot J_i^T \tag{23}$$

where i applies to any one of the components and the drops as well and where C_i is the total concentration of i per unit volume of microemulsion. The initial and boundary conditions associated with Eq. 23 are

$$\begin{aligned} C_i(x, 0) &= C_i^{\text{cap}}(0) \\ \frac{dC_i(0, t)}{dx} &= 0 \\ C_i(L, t) &= C_i^{\text{bulk}} \end{aligned} \tag{24}$$

where $C_i^{\text{cap}}(0)$ is the concentration of material initially present in the capillary tube, and C_i^{bulk} is the concentration of component i in the bulk solution. For drops, replace C_i by the dispersed phase volume, ϕ_d. Equation 23 is solved using the method of lines (Gaffney, 1983). We used the IMSL subroutine DPDES, which solves parabolic partial differential equations. This algorithm discretizes the space dimension using cubic Hermite polynomials, thus generating a series of first-order ordinary differential equations that are integrated in time. For all simulations, 100 evenly spaced grid points were used in the solution domain. Numerical solution generates the discrete profiles $C_i(x, t)$ and $\phi_d(x, t)$. These profiles are then integrated across the capillary tube length to yield their average values.

Experimental Details

The open capillary experimental setup is shown in Figure 1. This technique involves measuring the change in concentration of microemulsion in a small capillary tube whose open end is inserted into a bulk solution, which contains microemulsion of a different composition. The run is ended after a known time when the tube is removed from the bulk solution. The contents are analyzed to determine their composition. The initial compositions of capillary and bulk solution are also analyzed for each experiment.

The entire experimental assembly in Figure 1 is located in an air bath where the temperature is fixed at 25°C. The diffusion cell that contains the bulk solution is a glass jar with a plastic screw-on lid. The capillary tubes are secured vertically

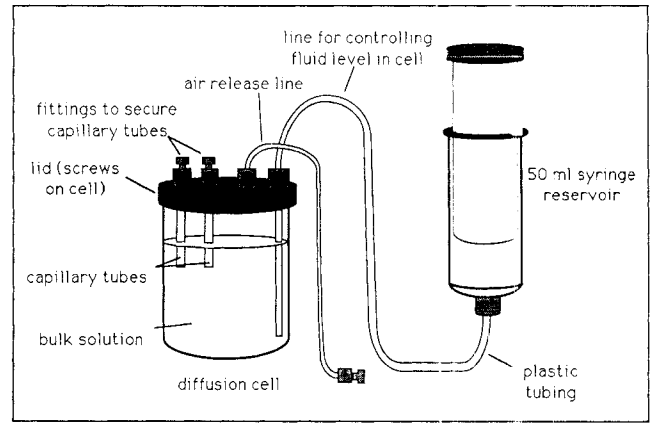

Figure 1. Open capillary experimental apparatus.

from the top at the lid. These tubes were 1.59 mm (1/16 in.) OD, 0.51 mm ID, and 3.1 cm in length. These dimensions are selected to minimize end effects. After cleaning, one end of each tube was flame-sealed to prevent evaporation of capillary solution during the experiment. Each tube was filled completely with solution using a microsyringe whose needle could be inserted inside the tube all the way to the closed end and care was taken that no bubbles remained in the filled tubes. After filling with capillary solution, the closed end was secured to the lid.

Because immersion and removal of the capillary tubes from bulk solution by hand could generate convection and skew the resulting concentration profiles, a procedure was developed to control the liquid level in the diffusion cell. A 50 mL syringe was connected by plastic tubing to the cell containing the bulk solution. By manually drawing back or depressing the syringe plunger, one can lower or raise the liquid level of bulk solution in the cell to minimize convection. Further details concerning the experimental apparatus and procedure can be found in McGreevy (1989).

Compositions of samples from this experiment were determined by gas chromatography, using a Hewlett-Packard 5890A gas chromatograph with auxiliary 3393A integrator and 7673A automatic sampler. The weight fraction of each component in unknown solutions was calculated using the ratio of its peak area to the peak area of the known initial capillary solution. This procedure of analyzing the composition of an unknown sample relative to that of a known standard is valid provided that the response factor, the ratio of peak area to weight fraction, is constant. We determined that this was the case for all components in the concentration ranges used in our diffusion experiments.

Materials and conditions

Both nonionic and ionic surfactant systems were selected for study. For the nonionic system, the predictions of the theory may be examined and compared to experimental data under conditions where bulk concentration and microstructure gradients exist, but where the gradient of electrical potential is everywhere zero. Then in the more complex case, modeling and experiments involving the ionic system allow us to study the situation where both composition and electrostatic gra-

dients exist. As shown in the Results section, the effect of the electrical potential gradient term on concentration profiles calculated from the theory is significant.

The nonionic microemulsion system studied in this paper is CO-850-water-benzene-phenol, where CO-850 is a blend of polyethoxylated nonylphenols manufactured by GAF Chemicals with an average ethylene oxide chain length of 20. Benzene obtained from Fisher Scientific and phenol from MCB Reagents were each of 99% purity and used as received. The phase diagram of this system has been discussed in McGreevy (1989). The clear, single-phase region from which solutions were chosen for experiments is located at the water-rich end of the diagram. The fourth component, phenol, is not essential in creating a stable single-phase microemulsion, but rather was chosen as an additive to this system to demonstrate countergradient diffusion. The ionic surfactant microemulsion system, also found in McGreevy (1989), is dodecyltrimethylammonium bromide (DTAB)-water-benzene-phenol. DTAB surfactant obtained from Aldrich Chemicals was of 99% purity and used without further purification. This system has similar phase behavior to the nonionic system, where the clear, single-phase region is at the water-rich end of its phase diagram.

The experiments reported here contact microemulsions dilute in the volume fraction of the dispersed phase (those solutions closest to the water vertex of the phase diagram) with solutions have a high composition of dispersed phase (those farthest from the water vertex but still in the clear region). Tracer self-diffusion measurements on the dilute microemulsion systems strongly suggest that the solution morphology in this region is in the form of droplets in a water-continuous phase. Therefore, a dilute microemulsion was chosen to be the capillary solution, while concentrated microemulsions of varying phenol content were assigned as the bulk solution in experiments. The locations on the phase diagram and the compositions of capillary and bulk solutions for the CO-850 and DTAB microemulsion systems are illustrated in Figures 2 and 3, respectively. It should be noted that no phase separation or formation of nonequilibrium structures occurred for any of the diffusion couples reported in this paper, as their diffusion paths are sufficiently removed from the phase boundaries.

The experimental conditions for each system were chosen such that the phenol content of the capillary solution was held constant at 0.5 wt. % while its concentration in the bulk was varied. In order to numerically simulate the diffusion experiment for the nonionic CO-850 microemulsion system, the following kinds of input parameters were required:

- Molecular self-diffusion data for water and phenol in water solvent
- Micelle or droplet diffusion coefficient for the capillary solution
- Partition coefficients for water, phenol, and benzene in the capillary solution to describe their dynamic equilibrium between the continuous and droplet phases
- Concentrations of water, phenol, and benzene in the capillary and bulk solutions
- Dispersed-phase volume fractions in the initial capillary and bulk solutions.

The self-diffusion data were obtained from the literature or determined by the Taylor dispersion technique (McGreevy,

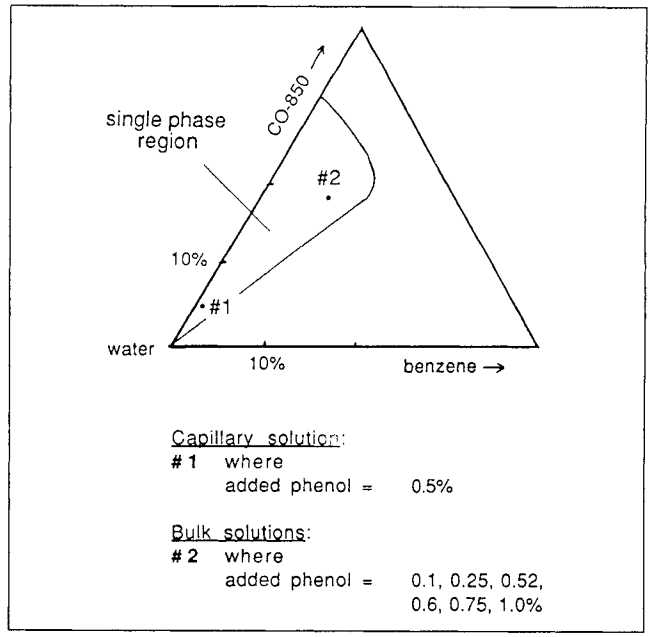

Figure 2. Phenol compositions in CO-850-water-benzene-phenol microemulsion system.

1989). Partitioning of each component between the continuous and droplet phases can be expressed by the dimensional partition factor β_i, which is defined in Eq. 7. Water is obviously found entirely in the continuous phase, so that β_w is equal to zero. Since hydrophobic benzene is solubilized almost completely inside the micelle cores, β_b was assigned a value of 10^6 for the simulations. Although this value may seem arbitrary, in fact our simulations show that if β_b is varied and given values as high as 10^{30}, there is no change in the predicted

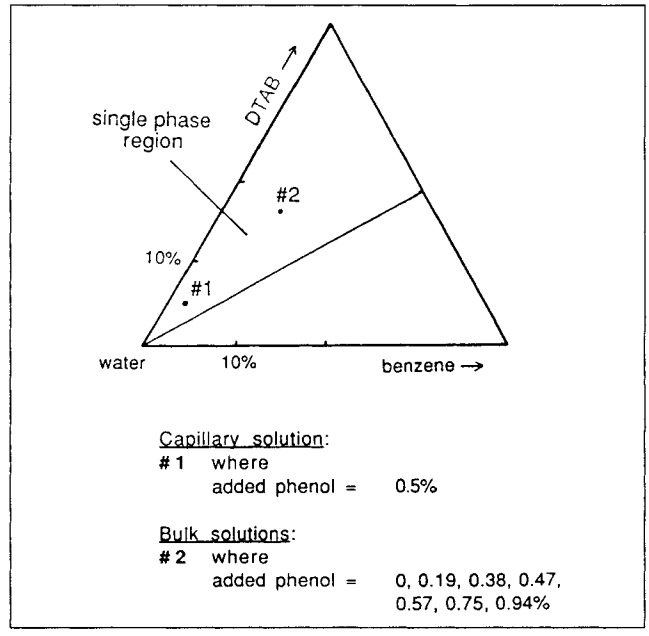

Figure 3. Phenol compositions in DTAB-water-benzene-phenol microemulsion system.

diffusion of benzene. Phenol, on the other hand, partitions between the aqueous and droplet phases (Kandori et al., 1989b). β_p was determined from tracer diffusion measurements by a procedure given in Kandori et al. (1989b), and its value is equal to 58.76. All solutions were made up by weight. By using densities of each component and assuming additive volumes, the volume fraction of all components could be determined. Dispersed-phase volume fraction ϕ_d equals the combined volume fractions of surfactant and benzene, which make up the droplet phase. A summary of input parameter values, which are used in diffusion simulations of the CO-850 microemulsion system, can be found in Table 1. In this table, the concentrations are converted to units of mol/mL.

For the ionic DTAB microemulsion system, numerical simulations also require molecular diffusion, micellar diffusion, and partitioning data for all components in the capillary solution. These factors have been determined in the same manner as those used in the nonionic simulations. However, additional parameters, which are not needed for simulating the nonionic system experiment, must be supplied for the ionic system case. As has been noted, these pertain to ionic surfactant aggregation as well as counterion dissociation behavior. They include:

- Surfactant monomer concentration in the continuous phase C_s^f
- Surfactant monomer diffusion coefficient D_s^f
- Valence of surfactant monomer Z_s^f
- Surfactant counterion diffusion coefficient D_c^f
- Valence of counterion Z_c^f
- Valence of component i Z_i
- Droplet interfacial area per surfactant head group A_s
- Surfactant partition factor β_s
- Degree of counterion dissociation from the droplets α.

The critical micelle concentration (CMC) for DTAB surfactant in water is 1.5×10^{-5} mol/mL (Mukerjee and Mysels, 1971). The effect of CMC decrease caused by the addition of phenol to this system has been studied by Kandori (unpublished results). Based on an interpolation of those data for our conditions, we estimate the surfactant monomer concentration for the four-component capillary solution to be 7.5×10^{-6} mol/mL. The diffusion coefficients of DTA^+ monomer and Br^- counterion in water at 25°C are 4.8×10^{-6} cm^2/s (Carlsson et al., 1989) and 2.084×10^{-5} cm^2/s (Cussler, 1984), respectively. As for surfactant head group area A_s, based on data and calculations from Kandori et al. (1989a) for the DTAB-water-benzene system, we used a value of 4.2×10^9 cm^2/mol of DTAB molecules for this parameter, which corresponds to approximately 70 Å^2 per surfactant head group absorbed at the droplet interface. Since Middleton (1988) reported that head group area for the similar DDAB surfactant system is about 68 Å^2, our value can be considered reasonable. From the method given in McGreevy (1989), the surfactant partition factor β_s was calculated to be 300.6 for the DTAB microemulsion used as the capillary solution. By a new procedure outlined in that work the dissociation degree α was determined to be 0.209. A summary of input parameter values, which are used in diffusion simulations of the DTAB microemulsion system, can be found in Table 2. All of the information needed for simulation of the diffusion of both nonionic and ionic surfactant microemulsions is now complete. The results of these simulations and experimental data are found in the next section.

Table 1. Parameter Values Used in Open Capillary Simulations of CO-850-Water-Benzene-Phenol System

Parameter	Value
β_b	10^6
β_p*	58.76
β_w	0
C_b^{bulk}	80.1×10^{-5}–80.7×10^{-5}mol/mL
C_p^{bulk}	1.07×10^{-5}–10.74×10^{-5}mol/mL
C_w^{bulk}	4.16×10^{-2}–4.2×10^{-2}mol/mL
$C_b^{cap}(0)$	6.42×10^{-5}mol/mL
$C_p^{cap}(0)$	5.31×10^{-5}mol/mL
$C_w^{cap}(0)$	5.26×10^{-2}mol/mL
D_p^{f*}	8.2×10^{-6}cm^2/s
D_w^{f**}	2.22×10^{-5}cm^2/s
D_m*	1.25×10^{-6}cm^2/s
ϕ_d^{bulk}	0.24–0.242
$\phi_d^{cap}(0)$	0.046
L (tube length)	3.1 cm
τ (time of exp.)	16.25 h (58,500 s)

*Taylor dispersion
**Mills (1971)

Results

CO-850-water-benzene-phenol system

Phenol Diffusion Results. Six separate experimental runs were performed. The initial capillary and bulk solution compositions of phenol, along with the resulting phenol capillary concentrations determined from theory and experiment at 16.25 h, are shown in Table 3. Both sets of results show a similar decreasing trend in final capillary concentration of phenol as the phenol content of the bulk solution is lowered. In run 1, both theory and experiment show that phenol concentration rises in the capillary when it is contacted with 1.0% phenol microemulsion in the bulk. Runs 5 and 6 show that phenol concentration decays inside the capillary tube when contacted with microemulsions of lower phenol content in the bulk. For each of these runs, phenol diffusion is occurring in the direction of the concentration gradient, as would be expected for simple liquids. However, the experimental data for runs 2, 3, and 4 reveal that during the period of measurement phenol concentration decreases in the capillary tube, despite the fact that the bulk solutions are more concentrated in phenol. Phenol diffusion in these runs is occurring against the concentration gradient. The results obtained from the theory also predict this countergradient diffusion of phenol for runs 3 and 4.

These same results for phenol are plotted in Figure 4 as normalized phenol concentration in the capillary tube as a function of bulk phenol concentration. Normalized concentration is defined as the difference between the resulting capillary concentration of material and the bulk concentration divided by the difference between the initial capillary concentration and the bulk concentration. The countergradient results are found for values of normalized concentration greater than unity. The discontinuity in normalized concentration of phenol shown in this plot occurs when the bulk concentration of phenol

Table 2. Parameter Values Used in Open Capillary Simulations of DTAB-Water-Benzene-Phenol System

Parameter	Value
α^*	0.209
A_s^{**}	4.2×10^9cm^2/mol
β_b	10^6
β_p^{***}	56.67
β_s^*	300.6
β_w	0
C_b^{bulk}	90.1×10^{-5}-91.0×10^{-5}mol/mL
C_p^{bulk}	0-10.0×10^{-5}mol/mL
C_w^{bulk}	4.16×10^{-2}-4.21×10^{-2}mol/mL
$C_b^{cap}(0)$	21.03×10^{-5}mol/mL
$C_p^{cap}(0)$	5.31×10^{-5}mol/mL
$C_w^{cap}(0)$	5.16×10^{-2}mol/mL
$C_s^{f\dagger}$	7.5×10^{-6}mol/mL
C_s	1.61×10^{-4}mol/mL
$D_c^{f\ddagger}$	2.084×10^{-5}cm^2/s
D_p^{f***}	7.5×10^{-6}cm^2/s
$D_s^{f\ddagger}$	4.8×10^{-6}cm^2/s
$D_w^{f\S}$	2.22×10^{-5}cm^2/s
D_m^{***}	3.82×10^{-7}cm^2/s
ϕ_d^{bulk}	0.248-0.25
$\phi_d^{cap}(0)$	0.068
L (tube length)	3.1 cm
τ (time of exp.)	16.25 h (58,500 s)
Z_c^f	−1
Z_s^f	+1

* McGreevy (1989) **Kandori et al. (1989) ***Taylor dispersion †Kandori (1990) ‡Cussler (1984) ‡Carlsson et al. (1989) §Mills (1971)

closely approaches that initially present in the capillary, 0.0532 M, which makes normalized concentration tend toward positive or negative infinity. These results show a very good agreement between theory and experiment.

Figure 5 shows simulated phenol concentration profiles within the capillary tube at various times, based on the conditions of run 3, which corresponds to the curve for 16.25 h. The node at the extreme right is positioned at the open end of the tube; its value is equal to bulk solution concentration of phenol, 0.063 M, or 0.6%, at all times. The remaining points inside the tube are initially at the same concentration of 0.0532 M and then change as a function of time. What occurs during the course of the experiment, according to this simulation, is quite remarkable. A well or minimum of phenol concentration develops within the tube near the open end. As the experiment proceeds, this well moves toward the middle of the tube and begins to broaden, as the curves for 16.25 and 69.4 h in Figure 5 illustrate. With further passage of time, the minimum in the center of the tube begins to disappear. The curves for 111.1, 166.7, and 278.8 h indicate that phenol concentration falls near the closed end of the tube. During these intermediate times phenol is being depleted near the closed end, while its concentration is building up near the open end. Ultimately, at very long times the phenol concentration in the capillary tube will become equal to its concentration in the bulk solution. The existence of a concentration minimum at the earlier times

Table 3. Open Capillary Simulation and Experimental Results of Phenol Concentrations for CO-850-Water-Benzene-Phenol System

	Initial Conditions (Phenol)		Results Time = 16.25 h (Phenol)	
Run	Bulk wt. %	Capillary wt. %	Theory wt. %	Exp. wt. %
1	1.0	0.5	0.543	0.520
2	0.75	0.5	0.515	0.485
3	0.6	0.5	0.498	0.481
4	0.52	0.5	0.489	0.478
5	0.25	0.5	0.461	0.437
6	0.1	0.5	0.445	0.426

implies that two opposing mechanisms of phenol diffusion are occurring in this system. We discuss these in more detail in the next section.

Water and Benzene Diffusion Results. The normalized capillary concentrations determined for water and benzene are shown in Figure 6 and 7 as a function of bulk phenol composition. All normalized concentrations in these plots are found to be less than unity. The results for these components (especially benzene) seem to show an even closer agreement between theory and experiment than that of the phenol case. This agreement is significant in light of the fact that the microemulsions contacted in diffusion experiments contain large concentration gradients of water and benzene. The nature of benzene and surfactant diffusion (which are associated primarily with droplets) in microemulsions is illustrated by Figure 8, which shows droplet volume fractions as a function of position in the tube for various times. By contrast with the phenol results, the droplet composition of the microemulsion in the capillary tube increases monotonically with position and time as that solution is contacted with one in the bulk having a

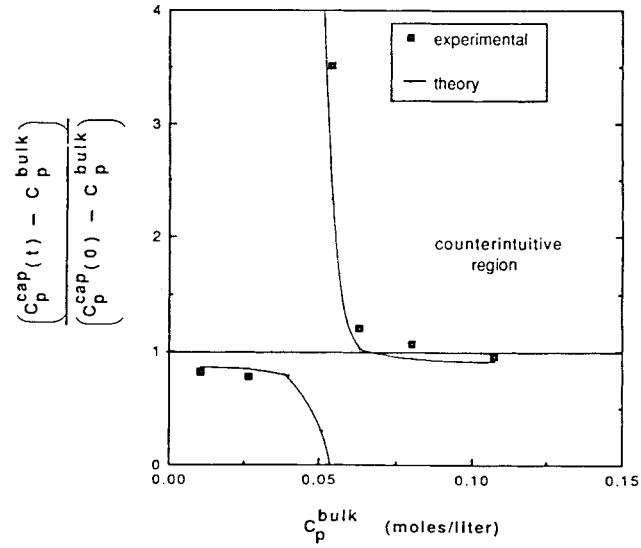

Figure 4. Normalized concentrations of phenol after 16.25 h, CO-850-water-benzene-phenol system.

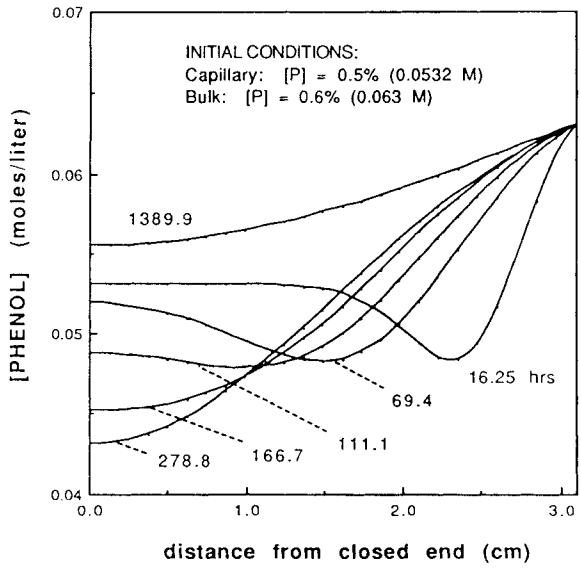

Figure 5. Simulated average phenol concentrations within capillary, CO-850-water-benzene-phenol system, as a function of time.

Conditions of run 3

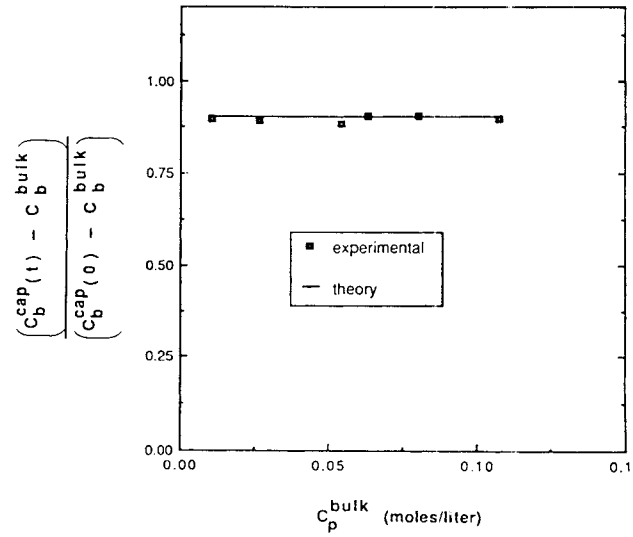

Figure 7. Normalized concentrations of benzene after 16.25 h, CO-850-water-benzene-phenol system.

much higher composition of dispersed phase (benzene and surfactant).

DTAB-water-benzene-phenol system

Phenol Diffusion Results. For the DTAB microemulsion system, seven experimental runs were performed. The initial compositions of phenol in the capillary and bulk solutions, along with the results generated from theory and experiments, are shown in Table 4. As the bulk solution concentration of phenol is lowered in runs 1-7, the resulting concentrations of phenol remaining in the capillary decrease monotonically according to theory and experimental results. For each run the theoretical predictions of phenol concentrations remaining in the capillary are slightly higher than those observed in experiments. As for simulations based on the theory, interesting results are noted in runs 3-6. In these runs, phenol diffusion is occurring from low-concentration regions in the bulk solution to higher concentration regions in the capillary solution, which we have referred to as counterintuitive or countergradient diffusion. This has the effect of concentrating the phenol in the capillary tube. For the experimental data in Table 4, run 4 also shows a clear countergradient diffusion effect, while runs 3 and 5, although not countergradient, nearly approach this behavior.

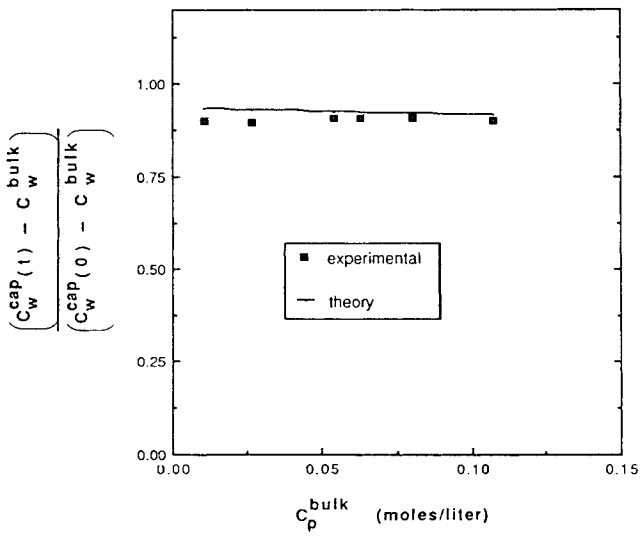

Figure 6. Normalized concentrations of water after 16.25 h, CO-850-water-benzene-phenol system.

These experimental and simulation results for phenol in the DTAB system are plotted in Figure 9 as normalized concentrations vs. bulk phenol concentrations. Countergradient results occur for this system when normalized concentrations are greater than unity or less than zero. This plot has a discontinuity at the point on the x axis where bulk concentration of phenol is equal to the initial capillary concentration of 0.052 M or 0.5%. Compare this plot to that of the CO-850 microemulsion system in Figure 4. For the nonionic system, phenol has a tendency to diffuse counterintuitively from low-concentration regions in the capillary solution to regions of higher concentration in the bulk solution. The DTAB system, as we have noted, shows just the opposite trend. The difference in behavior between the two systems has to do with the direction of the countergradient diffusion effect for phenol; it occurs toward the capillary tube for the ionic case and toward the bulk for the nonionic case. Because of this directional difference, their respective plots are roughly mirror images. In Figure 9, the trend predicted by the theory for the DTAB system is in fairly good agreement with the experimental results. By comparing these results with those obtained for the CO-850 system in Figure 4, we see that the agreement between theory and experiment is slightly better for the nonionic system. This slight disparity in the predictive accuracy of the diffusion theory is reasonable in light of the fact that more input parameters

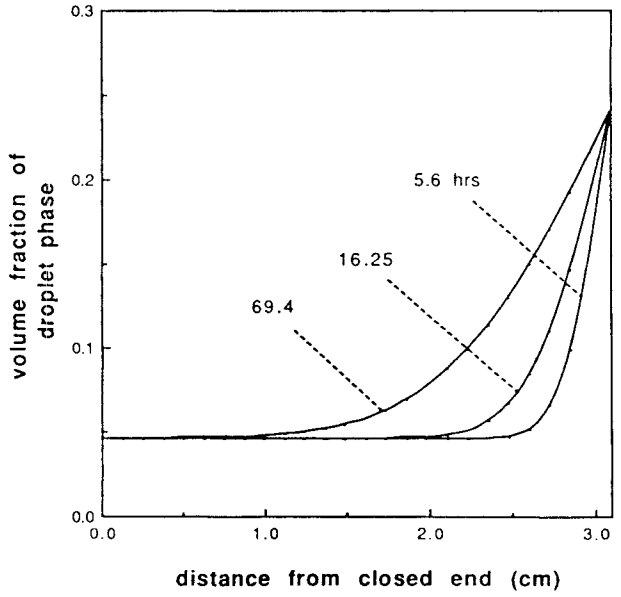

Figure 8. Simulated droplet volume fraction profiles within capillary for various times.

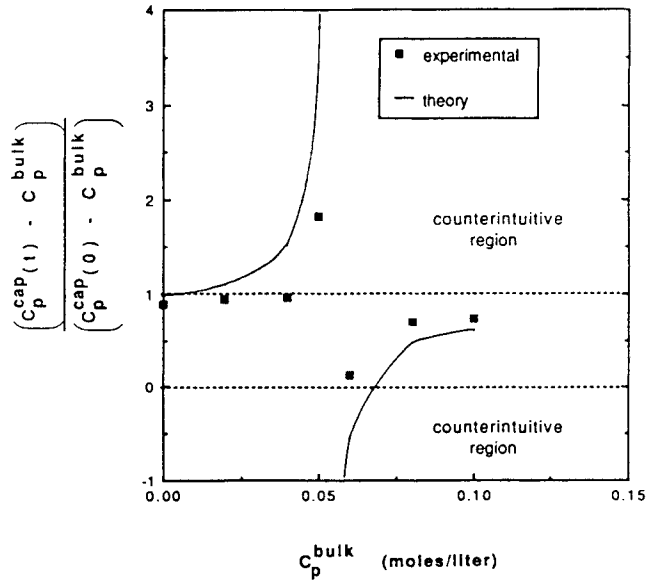

Figure 9. Normalized concentrations of phenol after 16.25 h, DTAB-water-benzene-phenol system.

are required to calculate diffusion for the ionic simulations. It should be emphasized that none of the parameters in either the nonionic or ionic simulations are adjustable. This provides a severe test of the predictive ability of the theory.

The next three figures show simulations based on the conditions of run 3 for the DTAB system. Figure 10 represents phenol concentration profiles within the capillary tube at various times. The time effect on phenol concentrations is fascinating: A concentration maximum develops and proceeds to the middle of the tube while broadening, as seen in the curves for 16.25 and 41.7 h. The maximum begins to disappear at 69.4 h as phenol concentrations increase near the closed end of the tube. A substantial buildup of phenol near the closed end continues with further passage of time, as the curve for 278.8 h illustrates. This accumulation of phenol in the capillary tube with increasing time is also seen in Figure 11, where phenol concentration, which is averaged across the tube length, is plotted as a function of time. A maximum is predicted to occur at approximately 300 h. After that point, phenol concentrations in the tube will drop until at very long times the bulk solution concentration of 0.06 M or 0.57% is reached. The decay in phenol concentration at long times is also illustrated by the curve for 833.3 h in Figure 10.

Figure 12 shows simulated phenol concentration profiles within the capillary tube as a function of droplet ionization degree α, one of the key parameters used in the simulation of ionic microemulsion diffusion. The curve for $\alpha = 0.209$ corresponds to the results obtained for run 3 of the DTAB system. The other curves correspond to solutions having the same microstructure and concentrations as those of run 3, except that the ionization degree parameter is varied. The curve for $\alpha = 0$ represents a nonionic system. There is a striking difference in concentration profiles between nonionic and ionic surfactant microemulsions. As we have noted, the ionic countergradient effect is for phenol diffusion to occur from low-concentration regions in the bulk solution to regions of higher concentration in the capillary, which causes phenol to become more concentrated inside the tube. We observe in these simulation results that as droplet ionization degree is raised, the counterintuitive effect becomes greater. The nonionic countergradient effect is just the opposite, leading to a net loss of phenol from the capillary into the bulk solution.

The influence of droplet ionization degree on diffusion is further illustrated in Figure 13, which shows simulated profiles of droplet volume fraction within the capillary for various ionization degrees. In considering this plot, it is obvious that the degree of counterion dissociation has a profound effect on the mobility of the droplets. The rate of migration of the dispersed phase from the bulk solution into the capillary is far greater for the DTAB system, corresponding to $\alpha = 0.209$, than for a nonionic system ($\alpha = 0$) with otherwise identical conditions. The electrical potential gradient $\nabla\psi$, which acts on the charged droplets, appears to be very influential in the diffusion of the dispersed phase.

Water and Benzene Diffusion Results. The normalized concentrations determined for water and benzene in the DTAB

Table 4. Open Capillary Simulation and Experimental Results of Phenol Concentrations for DTAB-Water-Benzene-Phenol System

Initial Conditions (Phenol)			Results Time = 16.25 h (Phenol)	
Run	Bulk wt. %	Capillary wt. %	Theory wt. %	Exp. wt. %
1	0.94	0.5	0.669	0.619
2	0.75	0.5	0.634	0.598
3	0.57	0.5	0.600	0.561
4	0.47	0.5	0.582	0.525
5	0.38	0.5	0.565	0.495
6	0.19	0.5	0.529	0.481
7	0	0.5	0.494	0.447

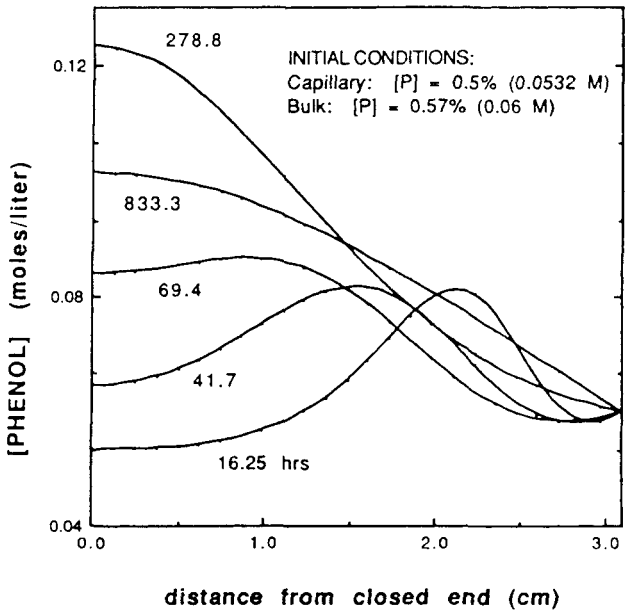

Figure 10. Simulated phenol concentration profiles within capillary, DTAB-water-benzene-phenol system for various times.

Conditions of run 3

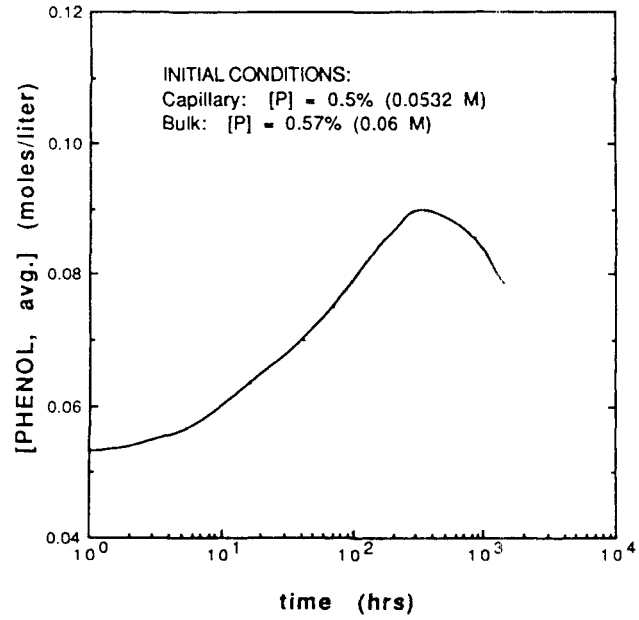

Figure 11. Simulated average phenol concentration profiles within capillary, DTAB-water-benzene-phenol system for various times.

Conditions of run 3

system are plotted in Figure 14 and 15 as a function of bulk phenol concentration. The results for these components show good agreement between theory and experiment for water, with fair agreement for the case of benzene. Consider the results for water diffusion for this system in Figure 14. This plot shows good agreement between theory and experiment, which suggests that our use of the $(1 - \phi_d)^2$ term in the diffusion theory as an obstruction factor is a reasonable description of continuous-phase diffusion in microemulsions. The additional nonadjustable parameters required to simulate diffusion of an ionic surfactant system and the extra sources of error that may be incurred, have a greater impact on the predicted concentrations of benzene than on water. Variations in the droplet ionization degree α, for example, have a strong effect on droplet diffusion and along with it the benzene concentrations, which are predicted by the theory. This factor alone would account for the discrepancy between theory and experiment found for benzene in Figure 15.

Discussion

In considering the CO-850 and DTAB system diffusion results in Tables 3 and 4, for every run the average phenol concentrations in the capillary are slightly lower than the values predicted by the theory of diffusion. Additional simulations showed that none of the parameters could be varied, either individually or as a group, in such a way that the theoretical predictions of phenol concentration could be lowered for all runs and brought closer to experimental values. After all data were obtained, a small error in the experimental procedure was discovered (McGreevy, 1989); its correction will raise experimental values 1 to 2% and improve the agreement with theoretical results.

The countergradient results observed for phenol in the non-ionic and ionic microemulsion systems are interesting, and an explanation for them will now be considered.

Based on numerous computer simulations, it was determined that the molecular diffusion coefficient D_i^f, the droplet diffusion coefficient D_m, and partition factor β_i are what distinguish the diffusion behavior of phenol in these systems from

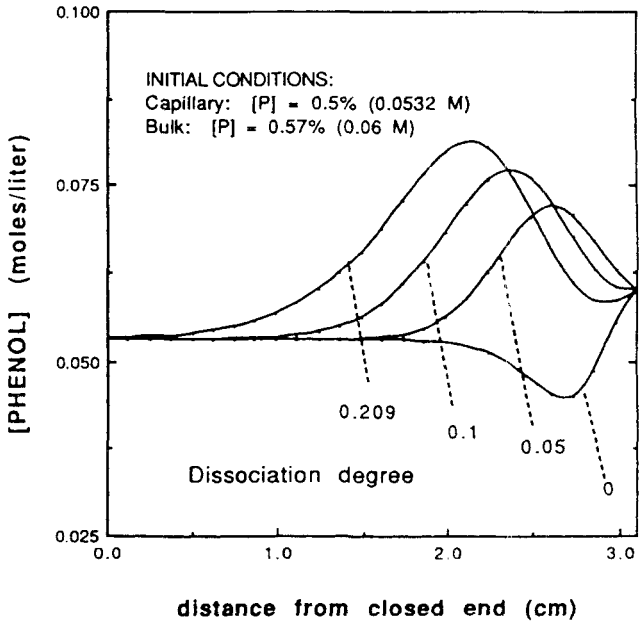

Figure 12. Simulated phenol concentration profiles within capillary, DTAB-water-benzene-phenol system for various droplet dissociation degrees.

Conditions of run 3

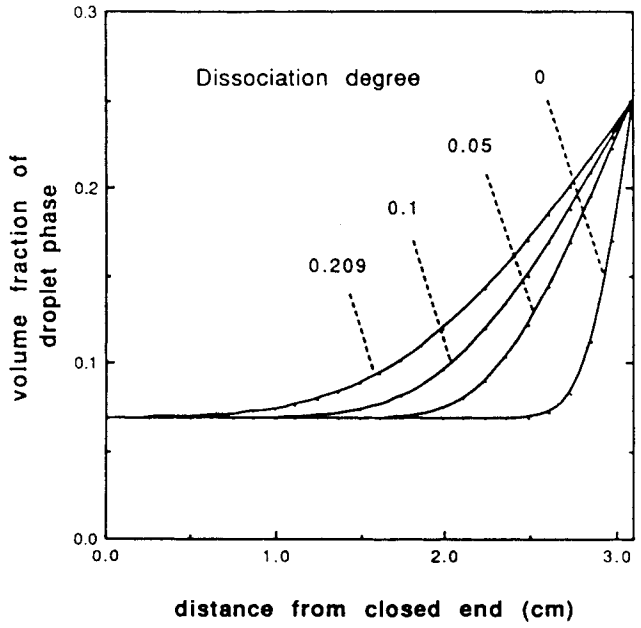

Figure 13. Simulated droplet volume fraction profiles within capillary for various droplet dissociation degrees.

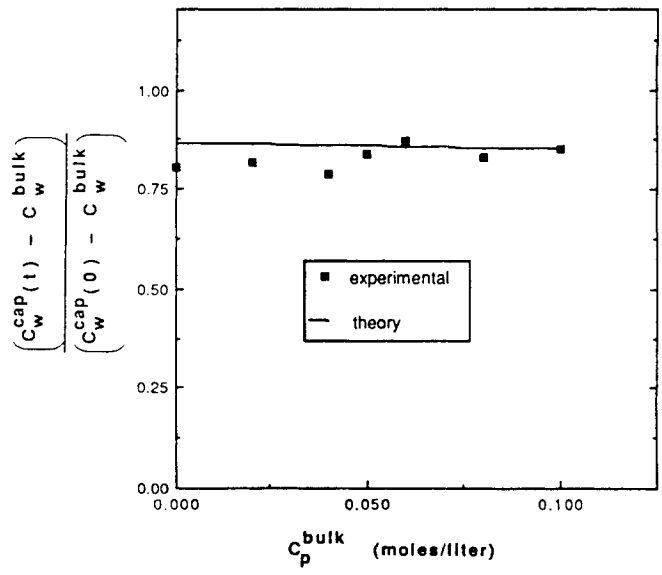

Figure 14. Normalized concentrations of water after 16.25 h, DTAB-water-benzene-phenol system.

that of water and benzene. For example, when the molecular diffusion coefficient and partition factor are each varied in simulations of the nonionic system while holding all other parameters constant, we found that values of D_i^f/D_m greater than 6.4 and β_i ranging from 5 to 70 lead to the countergradient diffusion of phenol. Both of these conditions are met by phenol for the capillary solution chosen in the CO-850 microemulsion system. The first condition associated with molecular diffusion is also met by water, but unlike phenol, water is found only in the continuous phase and does not partition in a manner that leads to countergradient diffusion. Neither of the two conditions is met by benzene or surfactant, which are associated almost completely with the droplets.

In the same microemulsion system, diffusion can occur according to molecular motion in the continuous phase and also as part of the slower Brownian droplets. The partition factor determines which of these two mechanisms will predominate for a given component. In the case of water, continuous-phase diffusion occurs, while benzene diffuses entirely with the droplets in this system. Phenol is found in both locations and thus has two mechanisms of diffusion occurring simultaneously. How this can explain the countergradient diffusion behavior of run 3 in the nonionic system, is illustrated in Figure 16. In these plots, the capillary concentration profile for phenol located in the continuous phase, along with the profile of the volume fraction of droplets, are shown here after 16.25 h. The portion of phenol that resides in the continuous phase is diffusing out of the capillary tube, while droplets are diffusing into the tube and carrying solubilized phenol with them. Because of the particular conditions that were selected for this experiment, these two mechanisms of diffusion are opposing one another, causing a minima in phenol concentration. Because the nature of droplet diffusion is slow relative to that in the continuous phase, the latter mechanism has a stronger influence on the mobility of phenol, which is directed from the capillary toward the bulk solution. Continuous-phase diffusion of phenol overcomes the effect of solubilized phenol diffusing from the bulk solution into the capillary. Thus, these competing mechanisms lead to a net diffusion behavior, which is counterintuitive.

These same two mechanism likewise exist in ionic surfactant microemulsions and can explain the net countergradient diffusion of phenol, which is directed into the capillary tube for the ionic system simulations and experiments. Consider the effect of ionization degree α on the mobility of the dispersed phase in Figure 13. By comparing the curves which correspond to $\alpha = 0$ and $\alpha = 0.209$, it is evident that droplet migration

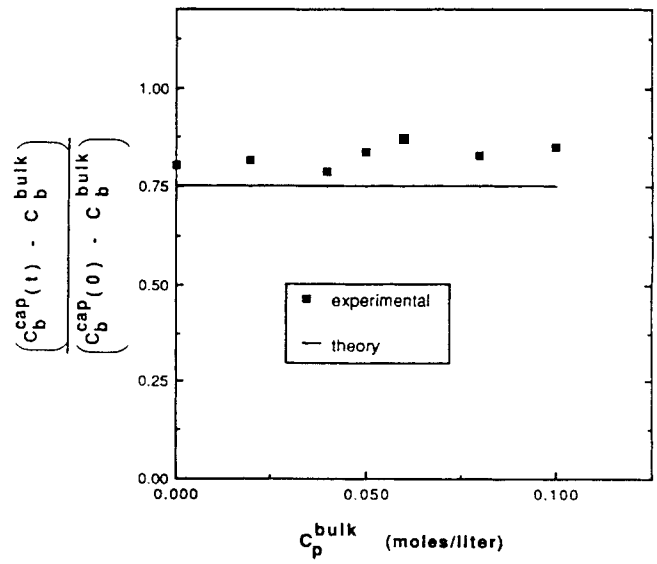

Figure 15. Normalized concentrations of benzene after 16.25 h, DTAB-water-benzene-phenol system.

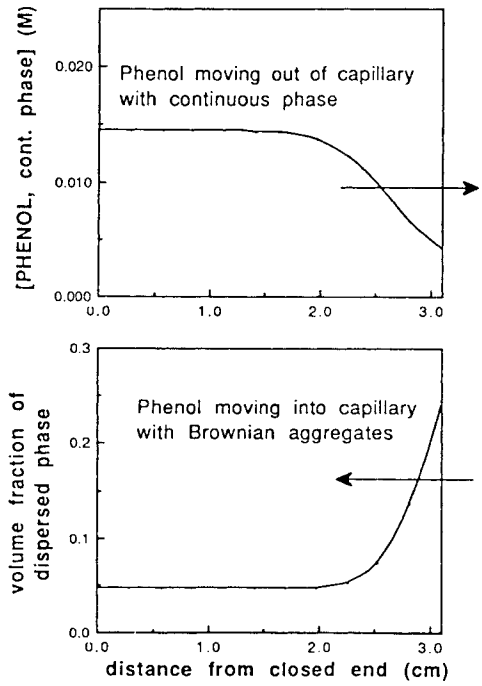

Figure 16. Two competing mechanisms of phenol diffusion: free diffusion in continuous phase, solubilized phenol diffusing with Brownian droplets.

into the capillary is dramatically higher for the latter case, which represents the DTAB system. For cationic DTAB surfactant, the droplets have a net positive charge due to the dissociation of negatively charged bromide counterions. Because the concentration of surfactant and of droplets is much greater in the bulk than in the capillary solution, there is a separation of charge when these solutions are brought into contact. An electric field arises to counteract this charge separation, and this field is responsible for the enhanced migration of charged droplets into the capillary tube. In the nonionic system, the effect of phenol migration out of the capillary tube via the continuous phase predominates over the effect of solubilized phenol diffusing into the tube with the droplets. But, for the DTAB system, the situation is reversed; the high rate of diffusion into the tube of droplets that carry solubilized phenol overcomes the outward diffusion of phenol in the continuous phase. The result is a larger than expected buildup of phenol in the capillary tube. This increasing mobility of the positively charged droplets compared with uncharged droplets provides the best explanation for the varying countergradient phenomena observed for phenol in the nonionic and ionic system cases.

Conclusions

This research has demonstrated that complex nonequilibrium diffusion phenomena in certain microemulsions can be adequately described by a droplet diffusion model that assumes local equilibrium. This is a key point not established by any previous study. The diffusion theory applies to both nonionic and ionic surfactant microemulsions. Gradients in the concentration of components i, droplet volume fraction, and (for the ionic system) electrical potential were present in these experiments, and the model clearly distinguishes the quantitative features of diffusion for each component. In particular, the theory is able to predict countergradient diffusion behavior for components, which partition between the continuous and droplet phases. This was verified in experiments by using phenol as the partitioning additive. Also, the differing countergradient behavior, which was observed for the nonionic and ionic systems, can be distinguished and explained by the diffusion theory. The open capillary experiment is demonstrated in this research to be extremely appropriate and useful for studying nonequilibrium diffusion behavior of microstructured solutions, whereas in the past its use was largely confined to equilibrium tracer diffusion studies.

A note of caution is appropriate, however. A careless interpretation of the countergradient results obtained for phenol will lead to a pitfall: If one used the analytical solution to the open capillary problem, he would calculate for phenol a negative value for the effective diffusion coefficient, a nonphysical result. Clearly, in order to adequately describe diffusion in microemulsions under nonequilibrium conditions, it is not sufficient to consider only concentration differences of a component in a diffusion couple. Knowledge of microstructure and electrostatic gradients as well as concentration gradients is a requirement for modeling diffusion in these systems.

Acknowledgment

This research was supported by the U.S. Department of Energy.

Notation

A_s = area per mole of surfactant head groups at droplet interface
C_i^{bulk} = concentration of component i in bulk solution
C_i^{cap} = concentration of component i in capillary solution
C_i^d = concentration of component i in microemulsion droplets
C_c^f = concentration of counterions in continuous phase of a microemulsion
C_i^f = concentration of component i in continuous phase of a microemulsion
C_s^f = concentration of surfactant monomer in continuous phase of a microemulsion
C_i = total concentration of component i in a solution or microemulsion
C_s = total concentration of bulk surfactant in solution
C_m = concentration of droplets in a microemulsion
CMC = critical micelle concentration
D_c^f = molecular diffusion coefficient of counterion
D_i^f = molecular diffusion coefficient of component i
D_s^f = molecular diffusion coefficient of surfactant monomer
D_m = micelle or droplet diffusion coefficient
J_d = flux of dispersed phase in a microemulsion
J_i^f = flux of component i in continuous phase of a microemulsion
J_c^f = flux of counterions in continuous phase of a microemulsion
J_s^f = flux of surfactant monomer in continuous phase of a microemulsion
J_m = flux of droplets in a microemulsion
J_{mi} = flux of component i associated with dispersed phase of a microemulsion
J_i^T = total flux of component i in a microemulsion
k = Boltzmann's constant
M = moles/liter
n = surfactant aggregation number
N_A = Avogadro's number
R = radius of micelle or droplet
T = temperature

Z_c^f = valence of counterion
Z_s^f = valence of surfactant monomer
Z_i = valence of component i
Z_m = net valence of micelle of droplet

Greek letters

α = degree of counterion dissociation from ionic surfactant aggregates
α_i = fraction of component i located in continuous phase of a microemulsion
β_i = partition factor for component i between dispersed and continuous phases
ϕ_d^{bulk} = dispersed phase volume fraction in bulk solution
ϕ_d^{cap} = dispersed phase volume fraction in capillary solution
ϕ_d = droplet or dispersed phase volume fraction
ψ = electrical potential

Literature Cited

Anderson, J. S., and K. Saddington, "The Use of Radioactive Isotopes in the Study of the Diffusion of Ions in Solution," *J. Chem. Soc.*, Supp. Issue No. 2, s381 (1949).

Armstrong, D. W., R. A. Menges, and S. M. Han, "Evaluation of Dye-Micelle Binding Constants Using Diffusion-Sensitive Band-Broadening Effects," *J. Coll. Int. Sci.*, **126**, 239 (1988).

Benton, W. J., K. H. Raney, and C. A. Miller, "Enhanced Video-microscopy of Phase Transitions and Diffusional Phenomena in Oil-Water-Nonionic Surfactant Systems," *J. Coll. Int. Sci.*, **110**, 363 (1986).

Bourrel, M., and R. S. Schechter, *Microemulsions and Related Systems: Formulation, Solvency, and Physical Properties*, Dekker, New York (1988).

Carlsson, A., G. Karlstrom, and B. Lindman, "Characterization of the Interaction between a Nonionic Polymer and a Cationic Surfactant by the Fourier Transform NMR Self-Diffusion Technique," *J. Phys. Chem.*, **93**, 3673 (1989).

Cussler, E. L., *Diffusion: Mass Transfer in Fluid Systems*, Cambridge Univ. Press, Cambridge (1984).

Ekwell, P., *Advances in Liquid Crystals*, G. H. Brown, ed., Academic Press, New York (1975).

Gaffney, P. W., "Using the Method of Lines Technique to Solve Initial Boundary Value Partial Differential Equations," *Scientific Computing*, IMACS, North-Holland (1983).

Huh, C., "Equilibrium of a Microemulsion that Coexists With Oil or Brine," *Soc. Pet. Eng. J.*, **23**(5), 829 (1983).

Kandori, K., R. J. McGreevy, and R. S. Schechter, "Solubilization of Phenol and Benzene in Cationic Micelles: Binding Sites and Effect on Structure," *J. Phys. Chem.*, **93**, 1506 (1989a).

Kandori, K., R. J. McGreevy, and R. S. Schechter, "Solubilization of Phenol in Polyethoxylated Nonionic Micelles," *J. Coll. Int. Sci.*, **132**, 395 (1989b).

Lam, A. C., and R. S. Schechter, "A Study of Diffusion and Electrical Conduction in Microemulsions," *J. Coll. Int. Sci.*, **120**, 42 (1987a).

Lam, A. C., and R. S. Schechter, "The Theory of Diffusion in Microemulsion," *J. Coll. Int. Sci.*, **120**, 56 (1987b).

Lindman, B., P. Stilbs, and M. E. Moseley, "Fourier Transform NMR Self-Diffusion and Microemulsion Structure," *J. Coll. Int. Sci.*, **83**, 569 (1981).

Luisi, P. L., and B. E. Straub, *Reverse Micelles*, Plenum, New York (1984).

McGreevy, R. J., "Tracer and Nonequilibrium Diffusion in Micellar and Microemulsion Systems," PhD Diss., Univ. Texas, Austin (1989).

Middleton, M., "Dielectric Properties and Structure of Oil-Continuous Microemulsions," PhD Diss., Univ. Texas, Austin (1988).

Miller, C. A., and P. Neogi, "Thermodynamics of Microemulsions: Combined Effects of Dispersion Entropy of Drops and Bending Energy of Surfactant Films," *AIChE J.*, **26**, 212 (Mar., 1980).

Mills, R., "Isotropic Self-Diffusion in Liquids," *Ber. Bunsenges Phys. Chem.*, **75**, 195 (1971).

Mukerjee, P., and K. J. Mysels, *Critical Micelle Concentrations of Aqueous Surfactant Systems*, NSRDS-NBS 36, U.S. Government Printing Office, Washington, D.C. (1971).

Overbeek, J. Th. G., "Microemulsions: a Field on the Border between Lyophobic and Lyophilic Colloids," *Farad. Discuss. Chem. Soc.*, **65**, 7 (1978).

Pratt, K. C., and W. A. Wakeham, "The Mutual Diffusion Coefficient of Ethanol-Water Mixtures: Determination by a Rapid, New Method," *Proc. Roy. Soc. Lond.*, **A336**, 393 (1974).

Raney, K. H., and C. A. Miller, "Diffusion Path Analysis of Dynamic Behavior of Oil-Water-Surfactant Systems," *AIChE J.*, **33**, 1791 (1987).

Ruckenstein, E., "The Origins of Thermodynamic Stability of Microemulsions," *Chem. Phys. Lett.*, **57**, 517 (1978).

Shulman, J. H., W. Stoeckenius, and L. M. Prince, "Mechanisms of Formation and Structure of Microemulsions by Electron Microscopy," *J. Phys. Chem.*, **63**, 1677 (1959).

Stilbs, P., and B. Lindman, "Aerosol OT Aggregation in Water and Hydrocarbon Solutions from NMR Self-Diffusion Measurements," *J. Coll. Int. Sci.*, **99**, 290 (1984).

Taylor, Sir G., "Dispersion of Soluble Matter in Solvent Flowing Slowly through a Tube," *Proc. Roy. Soc.*, **A219**, 186 (1953).

Manuscript received Dec. 28, 1989, and revision received Nov. 27, 1990.